

Exotics in a flux-tube perspective: hybrids and tetraquarks

Pedro Bicudo, Nuno Cardoso and Marco Cardoso

CFTP, Departamento de Física, Instituto Superior Técnico,
Universidade Técnica de Lisboa, Av. Rovisco Pais, 1049-001 Lisboa, Portugal

[arXiv:1107.1355] to be published in PRD, and [arXiv:1010.0281] PRD83,094010,2011

33rd International School on Nuclear Physics, Erice, Sicilia, 18th of September 2011

Abstract

The colour fields relevant for the hybrid and tetraquark systems are computed for static quarks in quenched SU(3) lattice QCD, with gauge invariant lattice operators, in a $24^3 \times 48$ lattice at $\beta = 6.2$. We generate our quenched configurations with GPUs. While at smaller distances the coulomb potential is expected to dominate, at larger distances it is expected that fundamental flux tubes, similar to the flux-tube between a quark and an antiquark, emerge and confine the quarks. We compute the square of the colour fields utilizing plaquettes, and locate the static sources with generalized Wilson loops and with APE smearing. The tetraquark system is well described by a double-Y-shaped flux-tube, with two Steiner points, but when quark-antiquark pairs are close enough the two junctions collapse and we have an X-shaped flux-tube, with one Steiner point. We also indicate how the hybrid excitations may affect the spectrum. And we indicate how to solve the Schrödinger equation for the tetraquark, and suggest that tetraquark resonances do exist.

Contents

1) Experimental results and motivation	3
2) Lattice technique to compute fields with the Wilson loop and the Plaquette	6
3) Lattice insight in the quark-antiquark flux tube	9
4) Theoretical study of excited mesons with chiral symmetry and flux tubes	11
5) Lattice computation of the Tetraquark fields	12
6) Theoretical computation of phase shifts for approximate 2-coordinate tetraquarks	17
7) Foreword	19

1) Experimental results and motivation

Exotic hadrons like glueballs, hybrids and multiquarks have been studied and searched for many years. For instance the tetraquark was initially proposed by Jaffe [1] as a bound state formed by two quarks and two antiquarks. Presently several observed resonances are tetraquark candidates. The most recent hybrid or tetraquark candidate has been reported by the Compass collaboration, the π^* with exotic parity 1^{-+} [2]. The most recent tetraquark candidates have been reported by the Belle Collaboration in May, the charged bottomonium $Z_b^+(10610)$ and $Z_b^+(10650)$ [3].

However a better understanding of quarks, gluons, flux tubes, tetraquarks is necessary to confirm or disprove the X, Y and possibly also light resonances candidates as tetraquark states.

Here we address the flux tube perspective. In the last years, the static tetraquark potential has been studied in Lattice QCD computations [4, 5, 6]. The authors concluded that when the quark-quark are well separated from the antiquark-antiquark, the tetraquark potential is consistent with One Gluon Exchange Coulomb potentials plus a four-body confining potential, suggesting the formation of a double-Y flux tube, composed of five linear fundamental flux tubes meeting in two Fermat points [7]. A Fermat, or Steiner, point is defined as a junction minimizing the total length of strings, where linear individual strings join at 120° angles. When a quark approaches an antiquark, the minimum potential changes to a sum of two quark-antiquark potentials, which indicates a two meson state. This is consistent with the triple flip-flop potential, minimizing the length, with either tetraquark flux tubes or meson-meson flux tubes, of thin flux tubes connecting the different quarks or antiquarks [8, 9].

Here we study the colour fields for the static tetraquark system, with the aim of observing the tetraquark flux tubes suggested by these static potential computations.

We also present theoretical studies utilizing our lattice results.

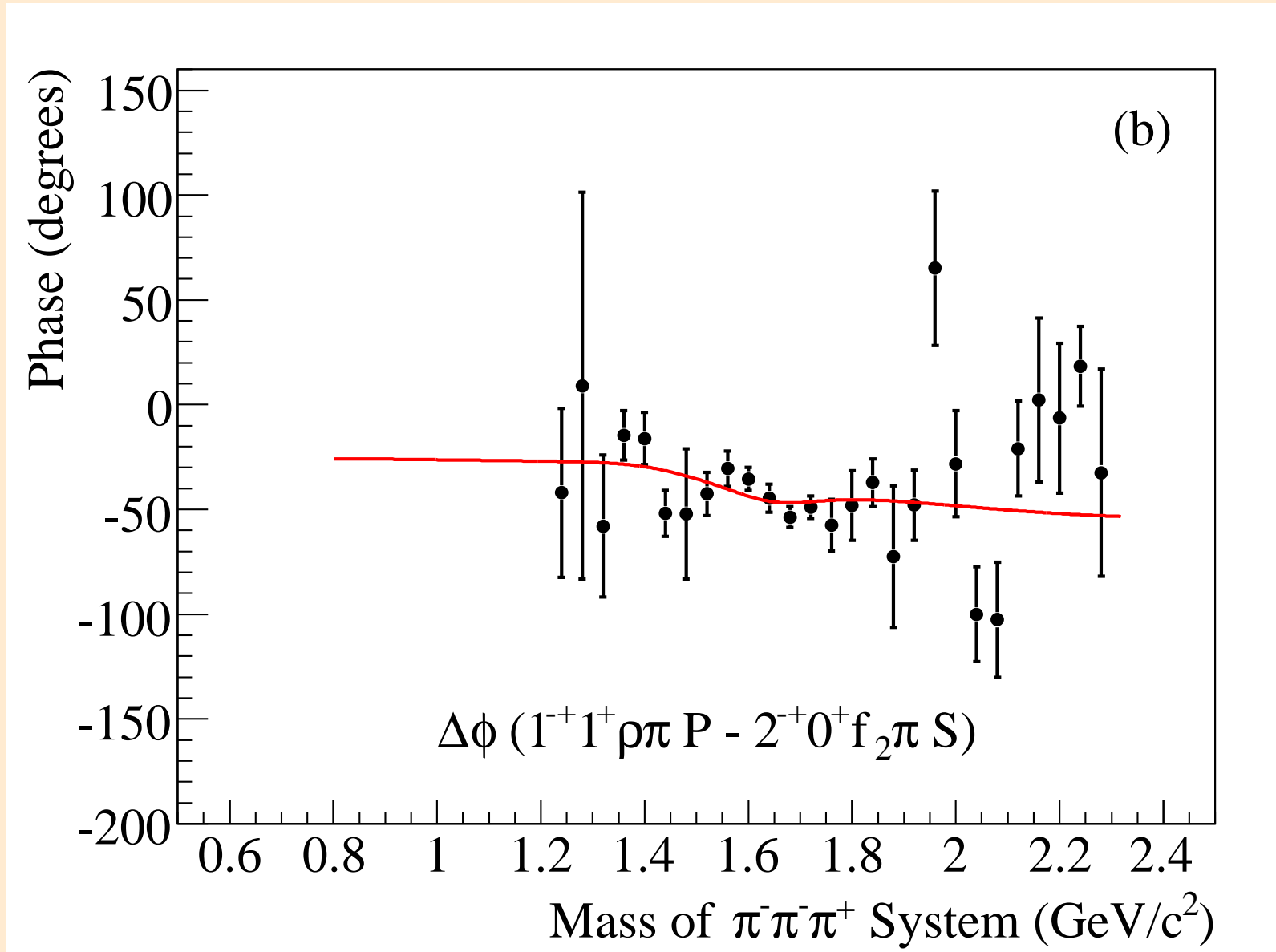


Figure 1: Compass exotic parity $\pi^1(1660)$ hybrid or tetraquark 1^{-+} candidate.

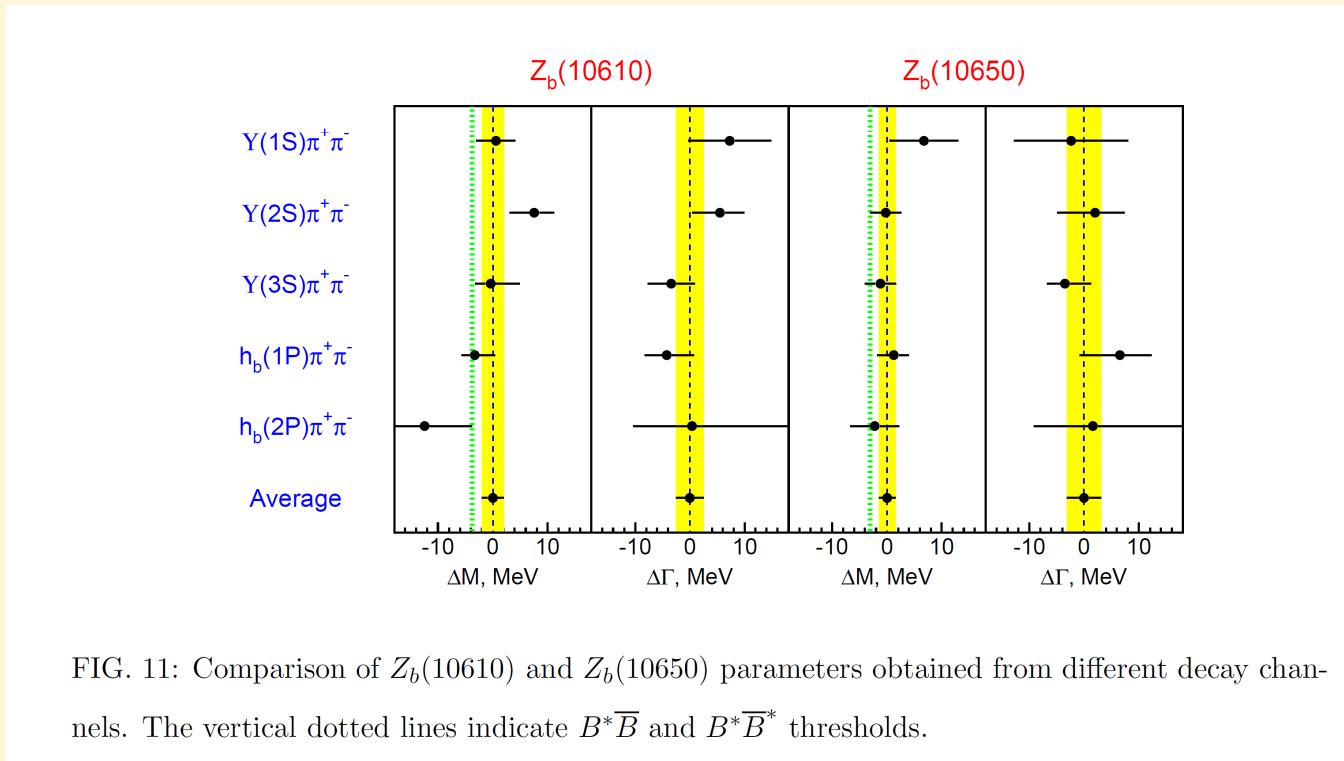


FIG. 11: Comparison of $Z_b(10610)$ and $Z_b(10650)$ parameters obtained from different decay channels. The vertical dotted lines indicate $B^*\bar{B}$ and $B^*\bar{B}^*$ thresholds.

Figure 2: Belle exotic flavour tetraquark candidates $Z_b^+(10610)$ and $Z_b^+(10650)$.

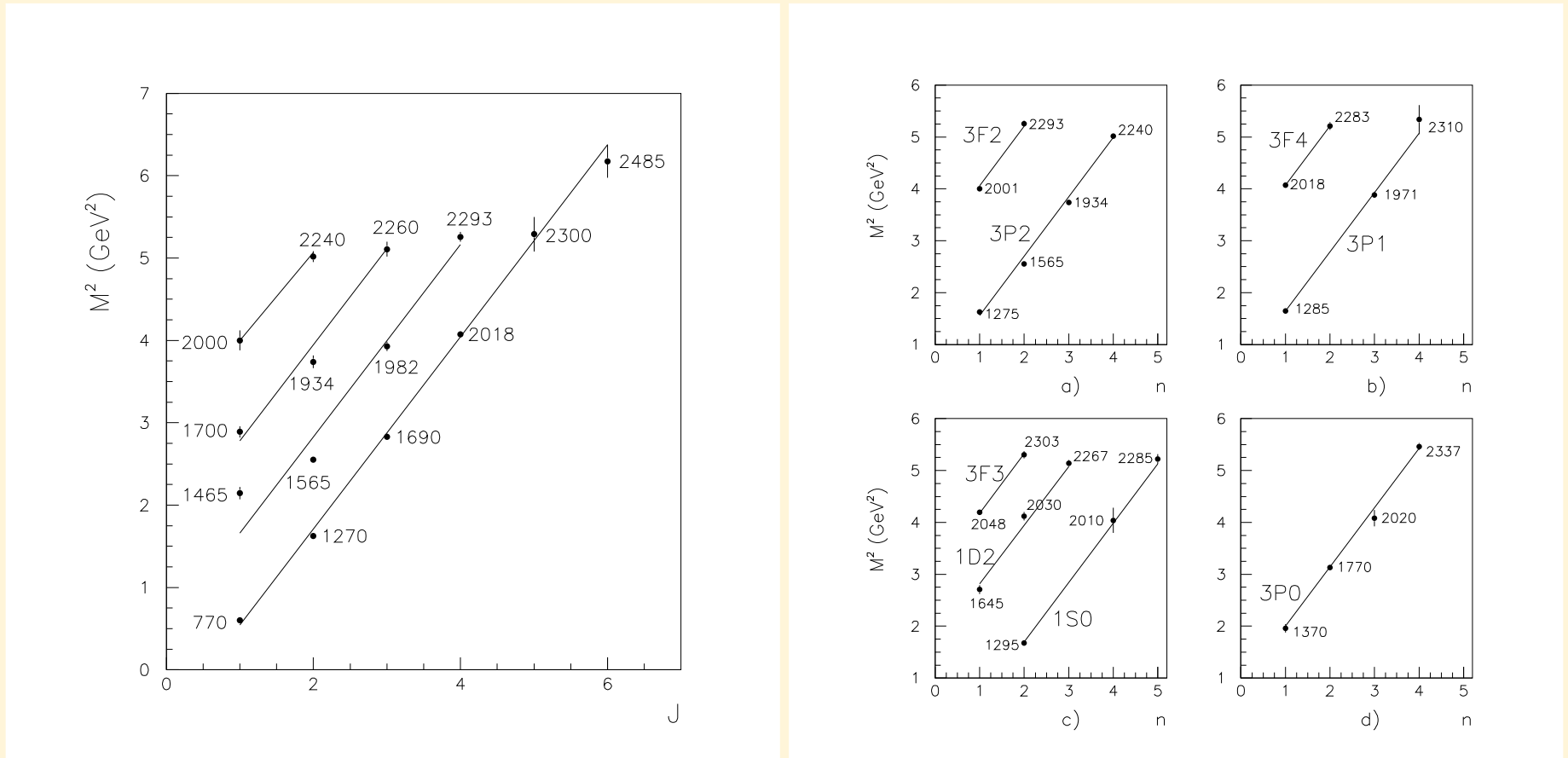


Figure 3: Excess of states in the meson excited spectrum observed by Crystal Barrel - LEAR, in CERN

2) Lattice technique to compute fields with the Wilson loop and the Plaquette

To impose a static tetraquark, we utilize the respective Wilson loop [4, 5] of Fig. 4, given by $W_{4Q} = \frac{1}{3} \text{Tr} (M_1 R_{12} M_2 L_{12})$, where

$$R_{12}^{aa'} = \frac{1}{2} \epsilon^{abc} \epsilon^{a'b'c'} R_1^{bb'} R_2^{cc'} ,$$

$$L_{12}^{aa'} = \frac{1}{2} \epsilon^{abc} \epsilon^{a'b'c'} L_1^{bb'} L_2^{cc'} .$$

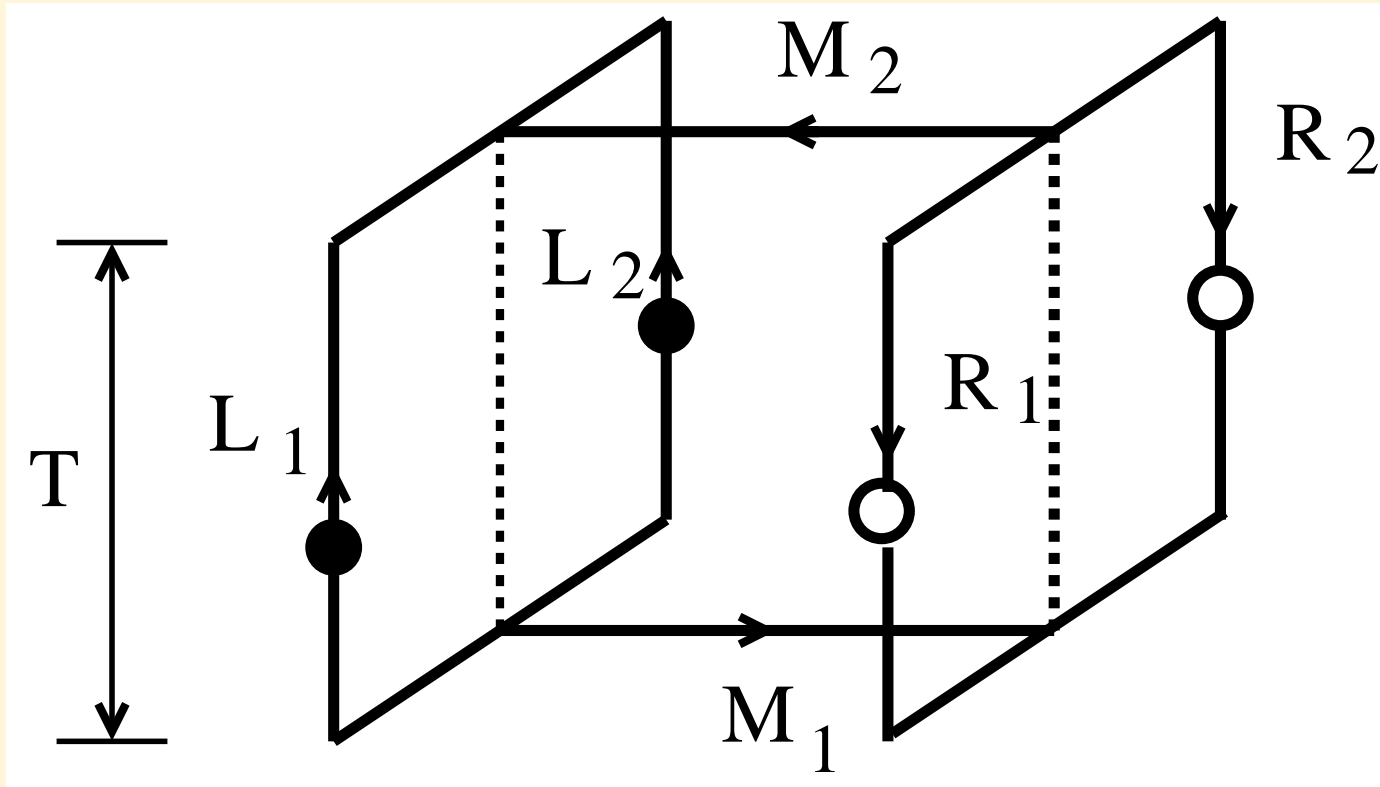


Figure 4: Tetraquark Wilson loop as defined by Alexandrou et al [4], and by Okiharu et al [5].

The chromoelectric and chromomagnetic fields on the lattice are given by the Wilson loop and plaquette expectation values,

$$\begin{aligned} \langle E_i^2(\mathbf{r}) \rangle &= \langle P(\mathbf{r})_{0i} \rangle - \frac{\langle W(r_1, r_2, T) P(\mathbf{r})_{0i} \rangle}{\langle W(r_1, r_2, T) \rangle} \\ \langle B_i^2(\mathbf{r}) \rangle &= \frac{\langle W(r_1, r_2, T) P(\mathbf{r})_{jk} \rangle}{\langle W(r_1, r_2, T) \rangle} - \langle P(\mathbf{r})_{jk} \rangle, \end{aligned} \quad (2)$$

where the jk indices of the plaquette complement the index i of the magnetic field, and where the plaquette at position

$\mathbf{r} = (x, y, z)$ is computed at $t = T/2$,

$$P_{\mu\nu}(\mathbf{r}) = 1 - \frac{1}{3} \text{Re Tr} [U_{\mu}(\mathbf{r})U_{\nu}(\mathbf{r} + \mu)U_{\mu}^{\dagger}(\mathbf{r} + \nu)U_{\nu}^{\dagger}(\mathbf{r})] . \quad (3)$$

The energy (\mathcal{H}) and lagrangian (\mathcal{L}) densities are then computed from the fields,

$$\langle \mathcal{H}(\mathbf{r}) \rangle = \frac{1}{2} (\langle \mathbf{E}^2(\mathbf{r}) \rangle + \langle \mathbf{B}^2(\mathbf{r}) \rangle) , \quad (4)$$

$$\langle \mathcal{L}(\mathbf{r}) \rangle = \frac{1}{2} (\langle \mathbf{E}^2(\mathbf{r}) \rangle - \langle \mathbf{B}^2(\mathbf{r}) \rangle) . \quad (5)$$

To compute the static field expectation value, we plot the expectation value $\langle E_i^2(\mathbf{r}) \rangle$ or $\langle B_i^2(\mathbf{r}) \rangle$ as a function of the temporal extent T of the Wilson loop. At sufficiently large T , the groundstate corresponding to the studied quantum numbers dominates, and the expectation value tends to a horizontal plateau. In order to improve the signal to noise ratio of the Wilson loop, we use 50 iterations of APE Smearing with $w = 0.2$ (as in [10]) in the spatial directions and one iteration of hypercubic blocking (HYP) in the temporal direction. [11], with $\alpha_1 = 0.75$, $\alpha_2 = 0.6$ and $\alpha_3 = 0.3$. Note that these two procedures are only applied to the Wilson Loop, not to the plaquette. To compute the fields, we fit the horizontal plateaux obtained for each point \mathbf{r} determined by the plaquette position, but we consider $z = 0$ for simplicity. For the distances r_1 and r_2 considered, we find in the range of $T \in [3, 12]$ in lattice units, horizontal plateaux with a $\chi^2 / \text{dof} \in [0.3, 2.0]$. We finally compute the error bars of the fields with the jackknife method.

3) Lattice insight in the quark-antiquark flux tube

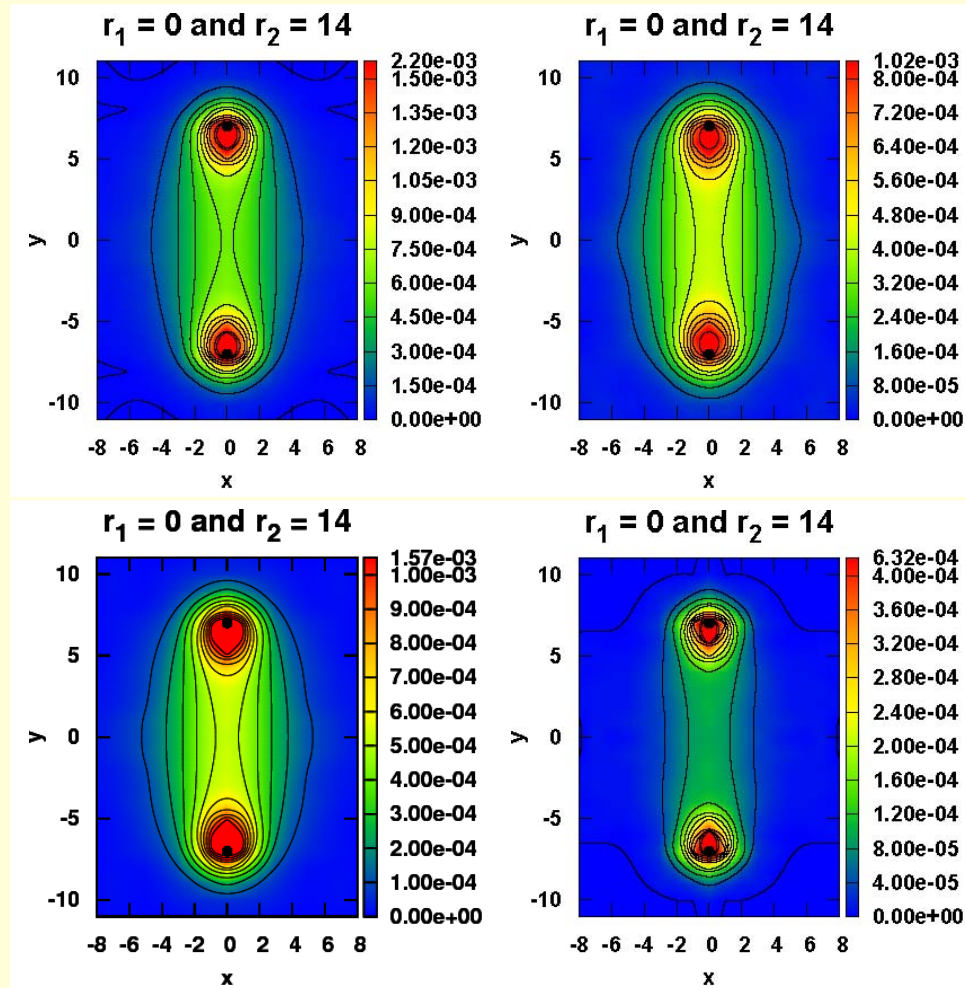


Figure 5: Density plot of the static quark-antiquark squared E and B, Lagrangian and Energy field densities for $r = 14$. The results are presented in lattice spacing units .

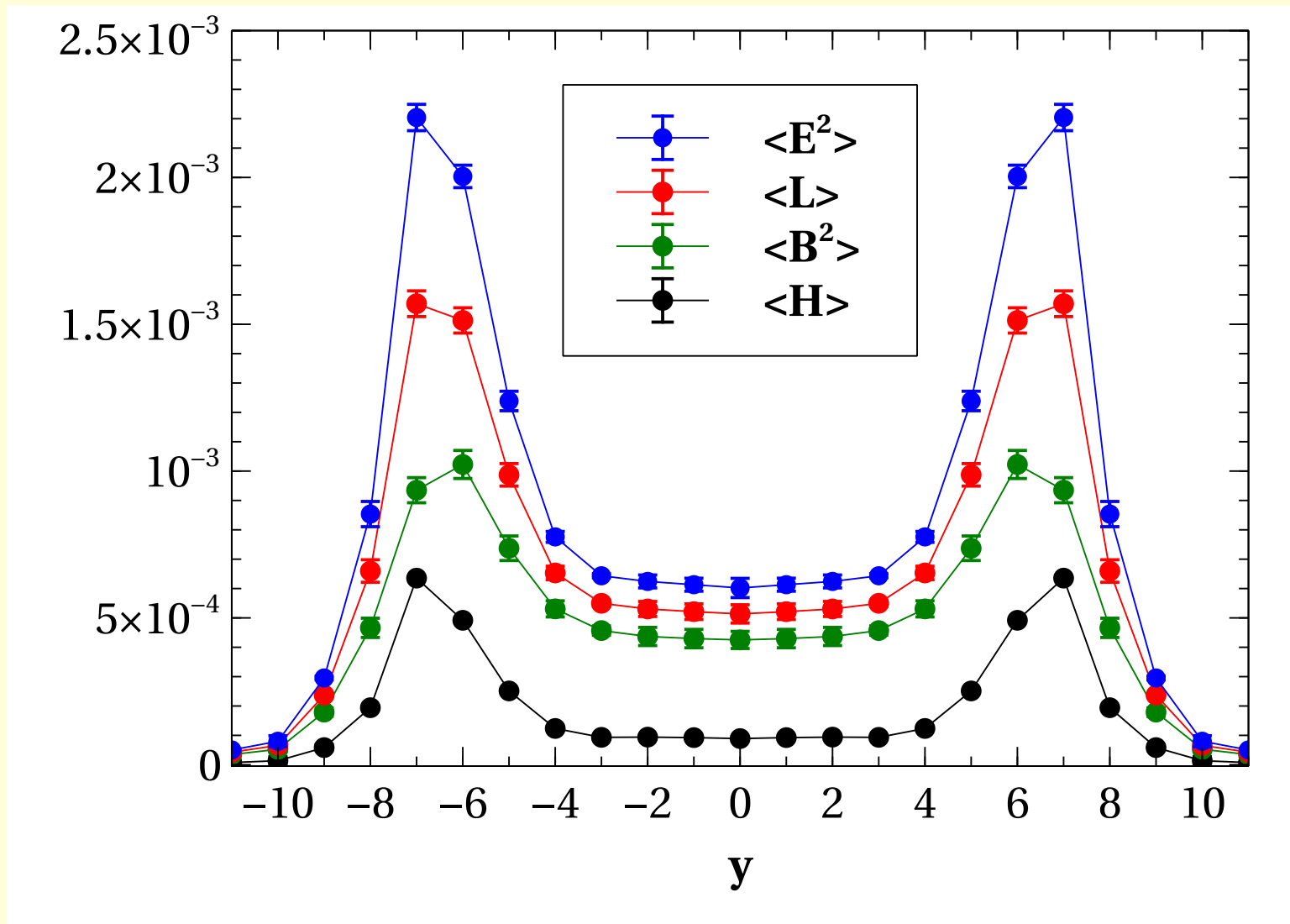


Figure 6: Cut of the fields in the longitudinal direction for $r = 14$. The results are presented in lattice spacing units.

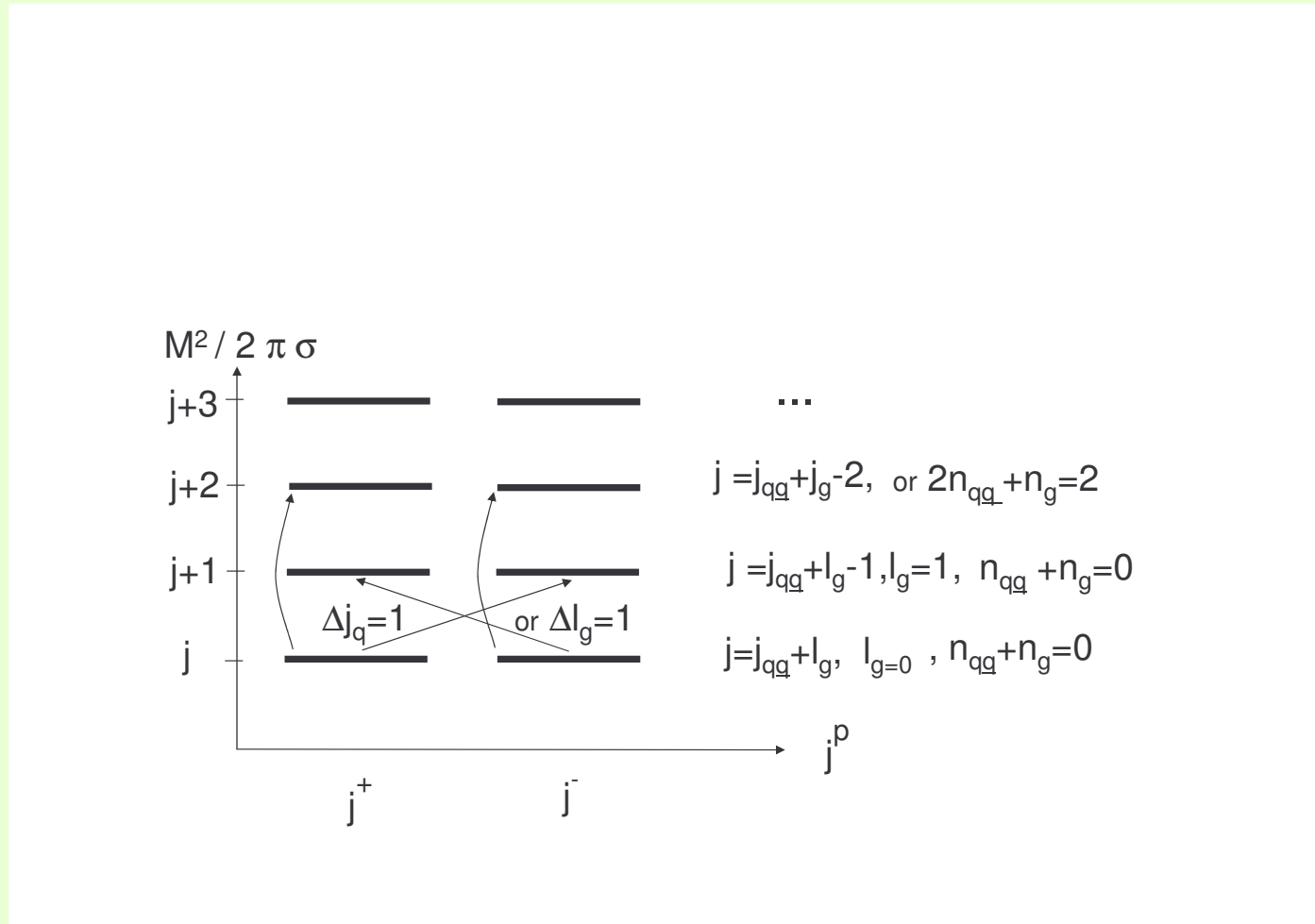


Figure 7: The combination of quark-antiquark angular excitations with flux tube rotation excitations .

4) Theoretical study of excited mesons with chiral symmetry and flux tubes

We utilize a quark model with chiral symmetry breaking and with a large number of radial and angular excitations, together with the hybrid excitations, to study the meson spectrum. We conjecture that the interplay of the two different quark ang flux tube excitations lead to a new principal quantum number in meson spectroscopy.

5) Lattice computation of the Tetraquark fields

In our simulations, the quarks are fixed at $(\pm r_1/2, -r_2/2, 0)$ and the antiquarks at $(\pm r_1/2, r_2/2, 0)$, with r_1 extending up to 8 lattice spacing units and r_2 extended up to 14 lattice spacing units, in order to include the relevant cases where $r_2 > \sqrt{3}r_1$. Notice that in the string picture, at the line $r_2 = \sqrt{3}r_1$ in our (r_1, r_2) parameter space, the transition between the double-Y, or butterfly, tetraquark geometry in Fig. ?? to the meson-meson geometry should occur. The results are presented only for the xy plane since the quarks are in this plane and the results with $z \neq 0$ are less interesting for this study. The flux tube fields can be seen in Fig. 11, 8 and 9. These figures exhibit clearly tetraquark double-Y, or butterfly, shaped flux tubes. The flux tubes have a finite width, and are not infinitely thin as in the string models inspiring the Fermat points and the triple flip-flop potential, but nevertheless the junctions are close to the Fermat points, thus justifying the use of string models for the quark confinement in constituent quark models.

In Fig. ??, we plot the chromoelectric field along the central flux tube, $\langle E_y^2 \rangle$ at $x = 0$, for $r_1 = 8, r_2 = 14$. As expected, the chromoelectric field along y is in agreement with the position of the Fermat points. The chromoelectric field along the $x = 0$ central axis is maximal close to the Fermat points situated at $x \simeq -4.69$ and at $x \simeq 4.69$, flattens in the middle of the flux tube. Outside the flux tube, the chromoelectric field is almost residual.

In Fig. 10, we compare the chromoelectric field for the tetraquark and the quark-antiquark system in the middle of the flux tube between the (di)quark and the (di)antiquark. As can be seen, for our larger distance $r_2 = 14$ where the source effects are small, the chromoelectric field is identical up to the error bars, and this confirms that the tetraquark flux tube is composed of a set of fundamental flux tubes with Fermat junctions.

To check which of the colour structures, tetraquark or meson-meson, produces the groundstate flux tube, we study the χ^2/dof of the T plateaux. The mixing between the tetraquark flux tube and the meson-meson flux tube is small, and it is possible to study clear tetraquark flux tubes even at relatively small quark-antiquark distances.

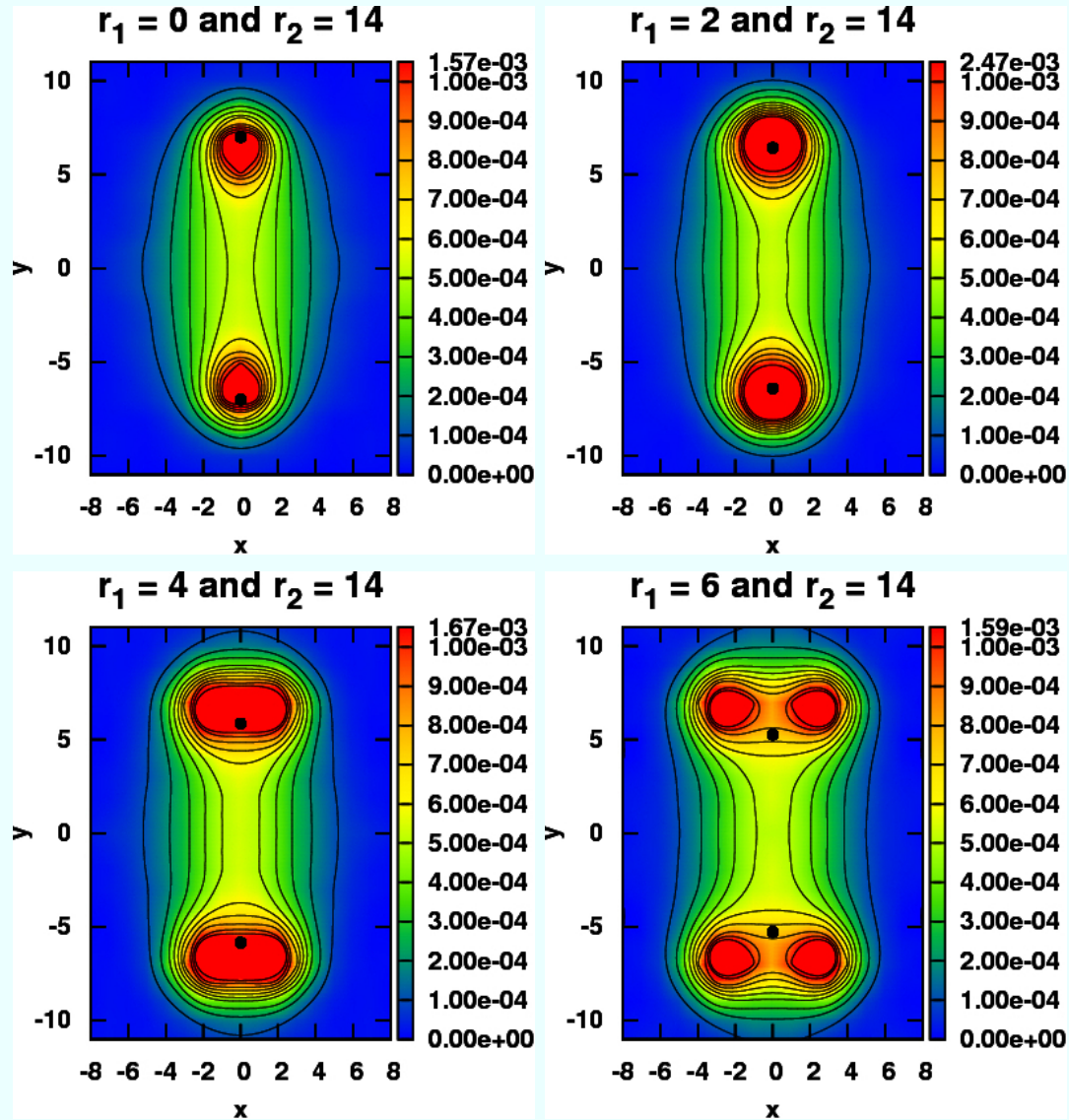


Figure 8: Lagrangian density for $r_2 = 14$ and r_1 from 0 to 6. The black dot points correspond to the Fermat points. The results are presented in lattice spacing units .

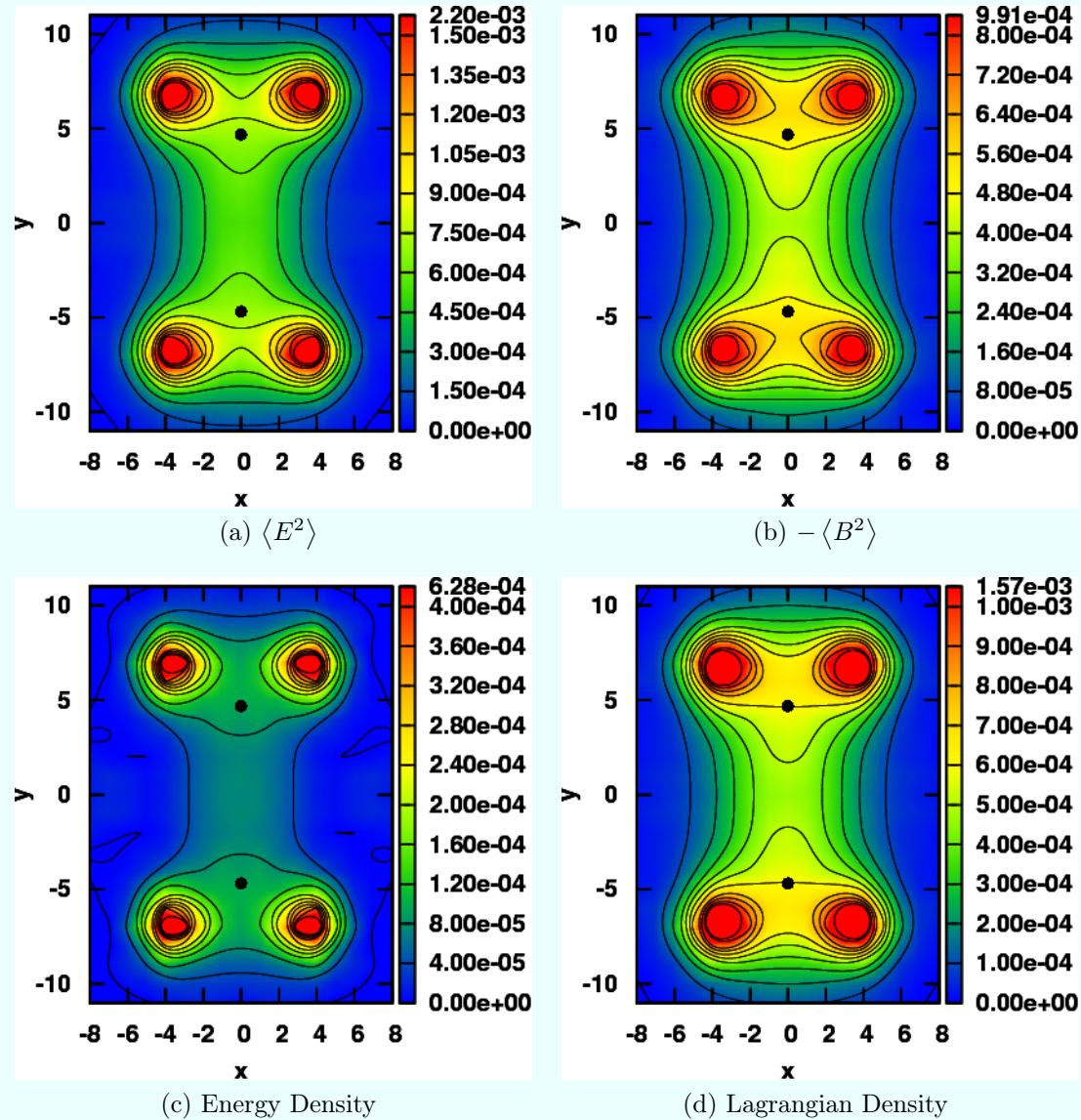


Figure 9: Colour fields, energy density and Lagrangian density for $r_1 = 8$ and $r_2 = 14$. The black dot points correspond to the Fermat points. The results are presented in lattice spacing units .

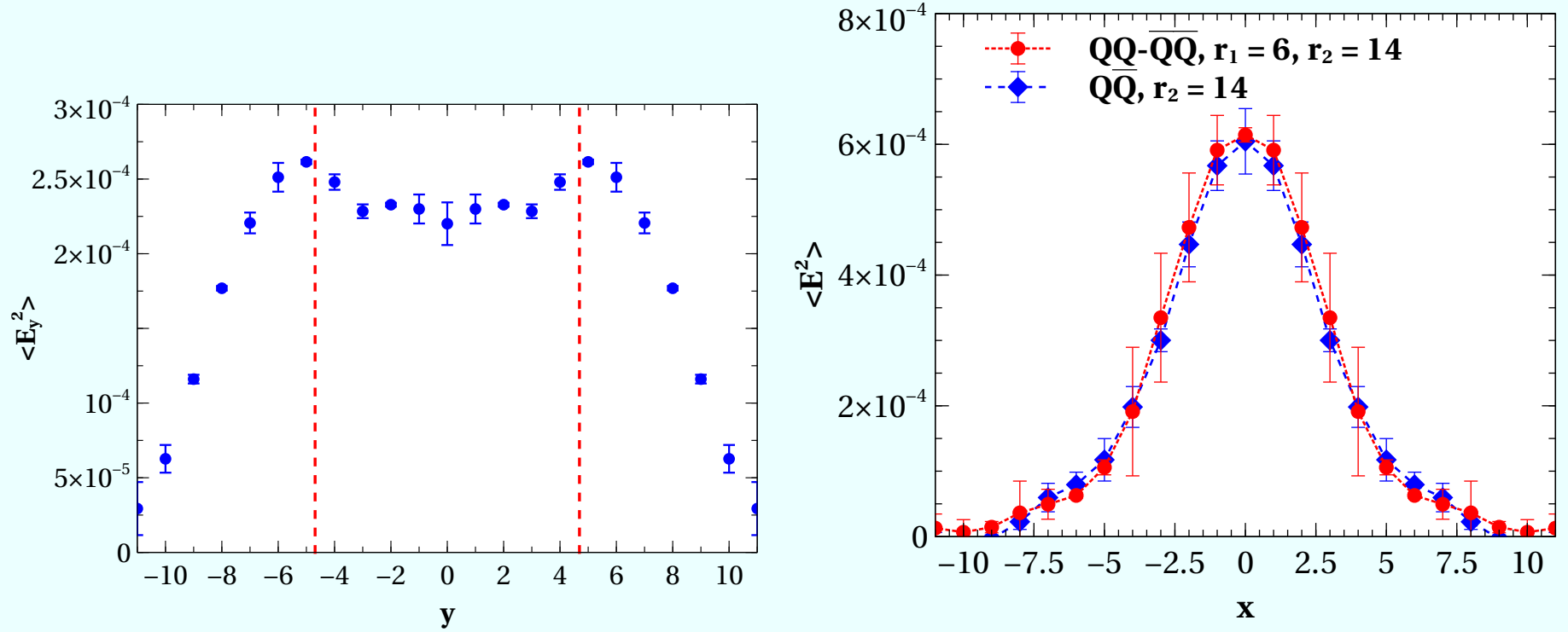


Figure 10: $\langle E_y^2 \rangle$ in the central axis $x = 0$ for $r_1 = 8$, $r_2 = 14$. We show with vertical dashed lines the location of the two Fermat points. Profile cut at $y = 0$ of the chromoelectric field for the tetraquark and quark-antiquark systems in the middle of the flux tube. The results are presented in lattice spacing units .

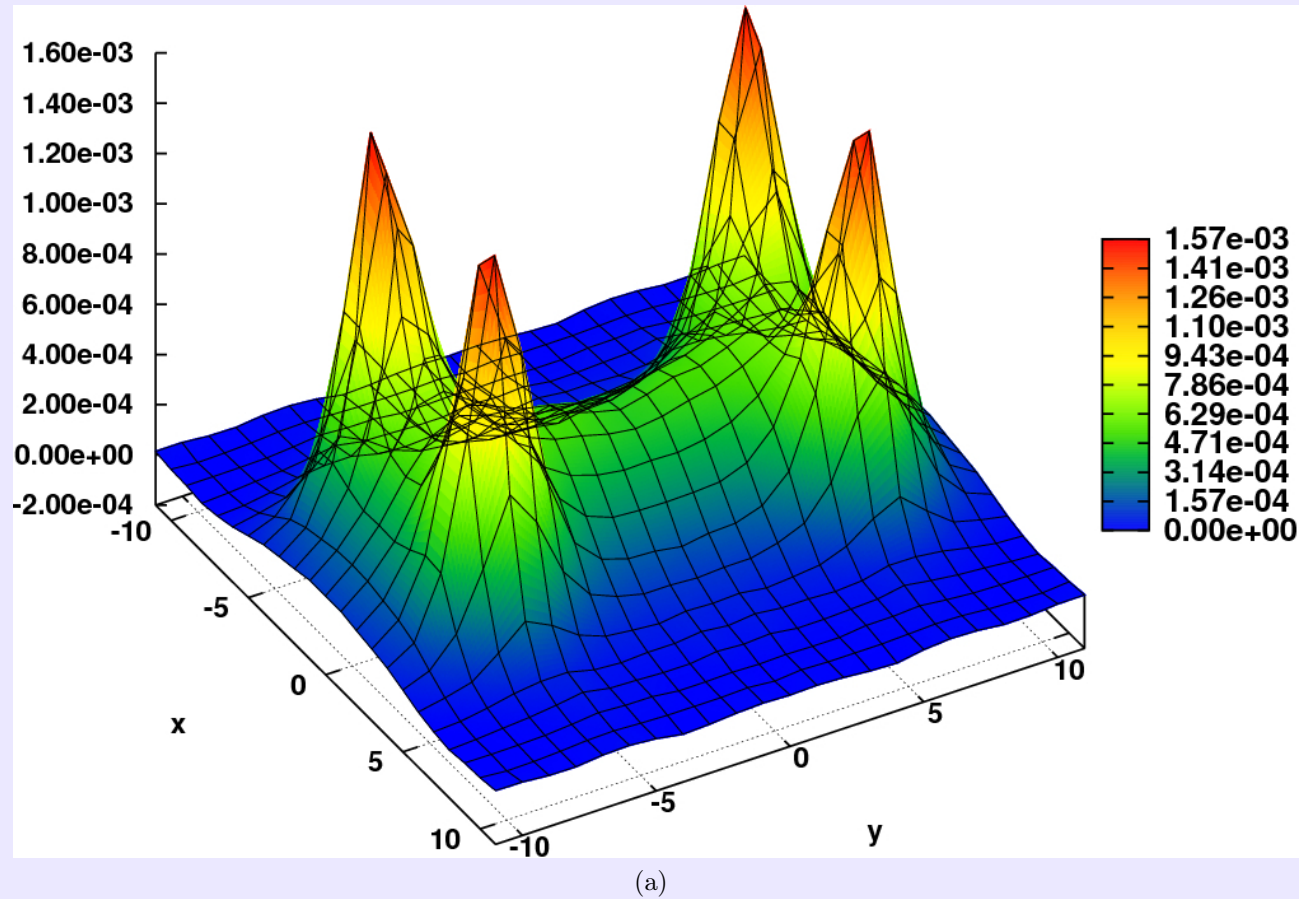


Figure 11: In the tetraquark flux tube (or string) model, the elementary flux tubes meet in two Fermat points, at an angle of $\alpha = 120^\circ$ to form a double-Y flux tube, except when this is impossible and the flux tube is X-shaped. Lagrangian density 3D plot for $r_1 = 8$, $r_2 = 14$. Here we show our results are presented in lattice spacing units .

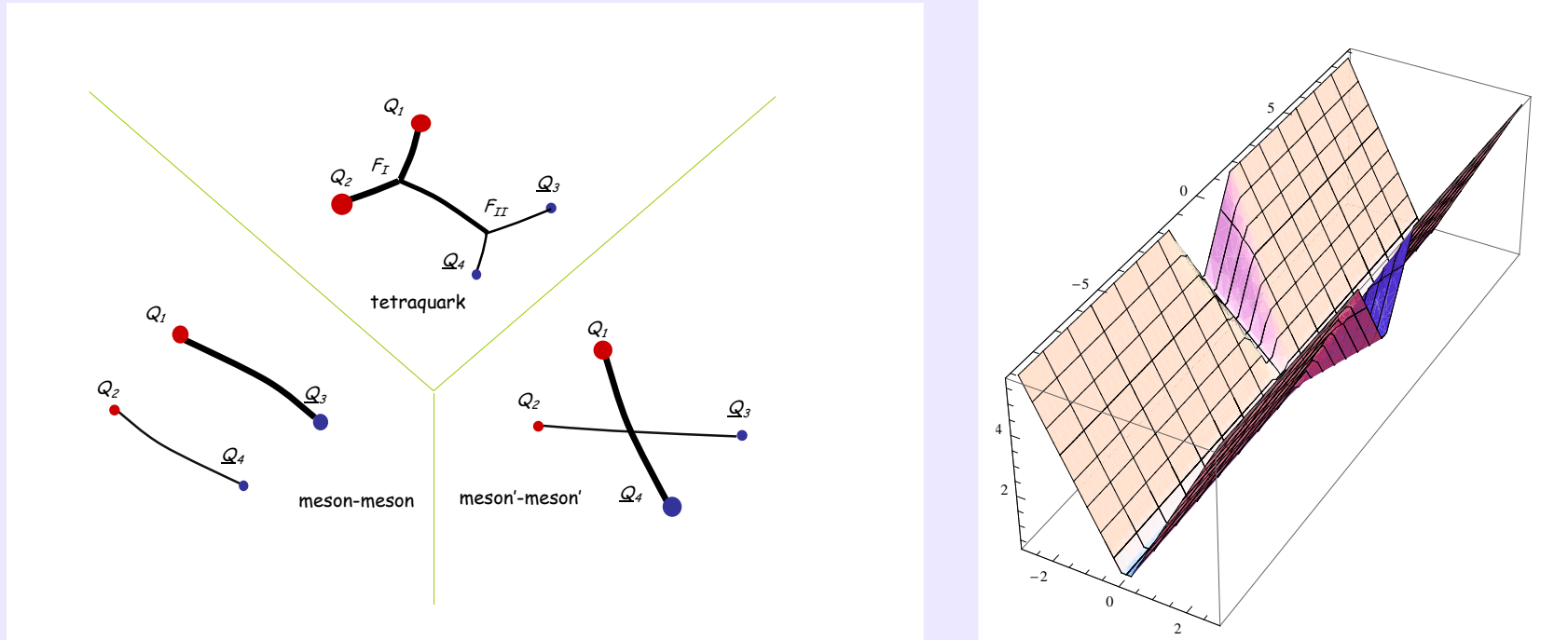


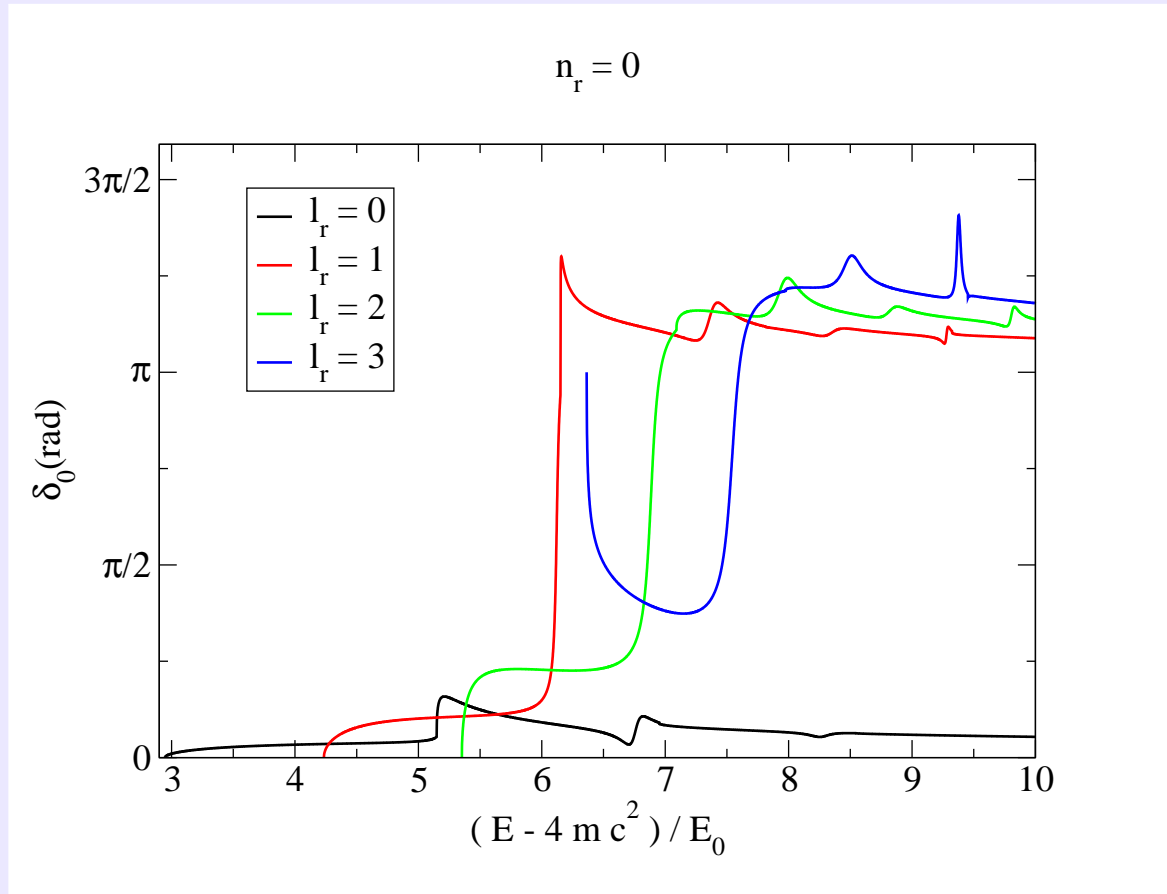
Figure 12: Triple flip-flop Potential potential. To the list of potentials to minimize including usually only two different meson pair potentials, we join another potential, the tetraquark potential. We also show the plot of our simplified flip-flop potential, as a function of the two radial variables r (compact) and ρ (open).

6) Theoretical computation of phase shifts for approximate 2-coordinate tretaquarks

Recently we developed a unitarized formalism to study tetraquarks using the triple flip-flop potential, which includes two meson-meson potentials and the tetraquark four-body potential.

We studied a simplified two-variable toy model and explore the analogy with a cherry in a glass, but a broken one where the cherry may escape from. It is quite interesting to have our system confined or compact in one variable and infinite in the other variable.

In this framework we solved the two-variable Schrödinger equation in configuration space. With the finite difference method, we compute the spectrum, we search for localized states and we attempt to compute phase shifts.



l_r	$(E - 4mc^2)/E_0$	Γ / E_0
1	6.116	0.037
2	6.855	0.131
3	7.462	0.352

Figure 13: Folding the confined coordinate with the solution of the meson Schrödinger equation then we can compute with a large precision the phase shifts. Here we illustrate the case of for $l_r = 0, 1, 2$ and 3 , with $n_r = 0$. We also show the decay widths as a function of l_r

We then applied the outgoing spherical wave method to compute in detail the phase shifts and to determine the decay widths. We fold the confined coordinate with the solution of the meson Schrödinger equation. We explored the model in the equal mass case, and we found narrow resonances. In particular the existence of two commuting angular momenta is responsible for our small decay widths.

7) Foreword

- The flux tubes remain interesting in Lattice QCD, our results support the string model of confinement, in particular for the tetraquark static potential [12].
- The mixing between the tetraquark and meson-meson flux-tubes is small, which may contribute for narrower tetraquark resonances.
- After our preliminary study of the approximate two-variable tetraquark, we are now moving on to the solutions of the Schrödinger equation for the tetraquark, in the full triple-flip-flop potential.
- We are now studying in more detail the flux tubes, in particular for the pentaquark.
- We will soon have codes for $SU(2)$, $SU(3)$, $SU(4)$, etc, available on our webpage,

<http://nemea.ist.utl.pt/~ptqcd/>

acknowledgments

This work was partly funded by the FCT contracts, PTDC/FIS/100968/2008, CERN/FP/109327/2009 and CERN/FP/116383/2010. Nuno Cardoso is also supported by FCT under the contract SFRH/BD/44416/2008.

References

- [1] R. L. Jaffe, “Multi-Quark Hadrons. 1. The Phenomenology of (2 Quark 2 anti-Quark) Mesons,” *Phys. Rev.*, vol. D15, p. 267, 1977.
- [2] M. Alekseev *et al.*, “Observation of a $J^{*}PC = 1^{-+}$ exotic resonance in diffractive dissociation of 190-GeV/c π^{-} into $\pi^{-} \pi^{-} \pi^{+}$,” *Phys.Rev.Lett.*, vol. 104, p. 241803, 2010. 7 page, 3 figures/ version 2 gives some more details, data unchanged/ version 3 updated authors, text shortened, data unchanged.
- [3] B. Collaboration, “Observation of two charged bottomonium-like resonances,” 2011.
- [4] C. Alexandrou and G. Koutsou, “The static tetraquark and pentaquark potentials,” *Phys. Rev.*, vol. D71, p. 014504, 2005.
- [5] F. Okiharu, H. Suganuma, and T. T. Takahashi, “The tetraquark potential and flip-flop in SU(3) lattice QCD,” *Phys. Rev.*, vol. D72, p. 014505, 2005.
- [6] V. Bornyakov, P. Boyko, M. Chernodub, and M. Polikarpov, “Interactions of confining strings in SU(3) gluodynamics,” 2005.
- [7] P. Bicudo and M. Cardoso, “Iterative method to compute the Fermat points and Fermat distances of multiquarks,” *Phys. Lett.*, vol. B674, pp. 98–102, 2009.
- [8] J. Vijande, A. Valcarce, and J. M. Richard, “Stability of multiquarks in a simple string model,” *Phys. Rev.*, vol. D76, p. 114013, 2007.
- [9] P. Bicudo and M. Cardoso, “Tetraquark resonances with the triple flip-flop potential, decays in the cherry in a broken glass approximation,” *Phys. Rev.*, vol. D83, p. 094010, 2011.
- [10] M. Cardoso, N. Cardoso, and P. Bicudo, “Lattice QCD computation of the colour fields for the static hybrid quark-gluon-antiquark system, and microscopic study of the Casimir scaling,” *Phys. Rev.*, vol. D81, p. 034504, 2010.
- [11] A. Hasenfratz and F. Knechtli, “Flavor symmetry and the static potential with hypercubic blocking,” *Phys. Rev. D*, vol. 64-3, p. 034504, 2001.
- [12] N. Cardoso, M. Cardoso, and P. Bicudo, “Colour Fields Computed in SU(3) Lattice QCD for the Static Tetraquark System,” 2011.